Piezoelectric actuator for a force-feedback application: preliminary evaluation

Gaston M'Boungui, Betty Lemaire-Semail, Frédéric Giraud

Piezoelectric actuator for a force-feedback application: preliminary evaluation

G. M'Boungui, B. Lemaire-Semail, F. Giraud

Laboratoire d'Electrotechnique et d'Electronique de Puissance de Lille

IRCICA

Abstract

As a solution to the lack of compactness and simplicity often encountered in haptic interfaces, we propose a device based on friction coefficient control principle. This device includes polarised piezoceramics well adjusted and glued to a 64x38x3 mm copper-beryllium plate supported by four legs. Then, properly energised around a resonant frequency, with legs at antinodes, a stationary wave is created in the plate. Variable friction forces between the legs and the plane substrate are created by the control of the wave amplitude, according to electro-active lubrication. So the user obtains force feedback by holding the plate, and moving it on a plane substrate, as he could do with a mouse interface. Preliminary psychophysical evaluation trends to assess the validity of the device as a force feedback interface.

KEYWORDS: piezoelectric actuator, force feedback, electro-active lubrication, psychophysical evaluation

1 INTRODUCTION

Many of the tasks in our daily life may be performed with greater efficiency and speed with haptic (tactile and force feedback rendering) assistance. Consequently, the use of force feedback to enhance interactive graphics has often been discussed since it's an area of growing interest from the research community and various devices of this field have been developed for many years. Nevertheless force feedback interfaces available are generally complex using a broad range of technologies, especially DC motors. So, as a motivation, in our research we aimed to design a compact and simple force feedback device.

This work presents design and implementation of our proposal which is a passive 2Dof device able to provide different resistant feeling sensations when a user moves it. To realise such a system, we chose to use active lubrication effect [1] induced by piezoelectric actuator. We also introduce preliminary evaluation of the system in use toward its qualification for force feedback rendering.

The actuator will first be described: it's based on a vibrating plate fitted with four legs. Then, the principle of active lubrication is reminded in that specific case which leads to a global control of adjustable friction coefficient between the plate and its plan support. This effect is underlined through simulation and experimental results about reactive force obtained with the device. At last, a psychophysical test is described and its results presented.

Rue Halley, 59655 Villeneuve d'Ascq cédex
Gaston.Mboungui@polytech-lille.fr
Betty.Semail@polytech-lille.fr
Frederic.Giraud@polytech-lille.fr

2 DEVICE

Figure 1 schematically shows the proposed structure. A set of PZT polarised piezo-ceramics of 12x12mm are glued on the upside of a cupper-beryllium substrate whose size is 64x38x3 mm. Considering this polarisation, piezo-ceramics electrode are conveniently supplied by a sinusoidal voltage of some ten Volts to create a standing wave using the piezoelectricity inverse effect with 40.7 kHz as driving frequency (resonant frequency). As a result, fig.2 shows an experimental mapping of the standing waveform obtained.

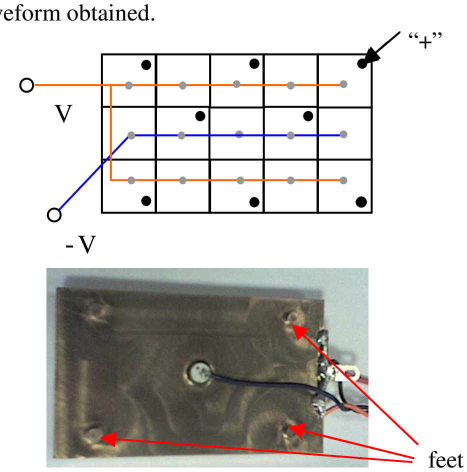

Fig.1: up scheme and down view of the actuator

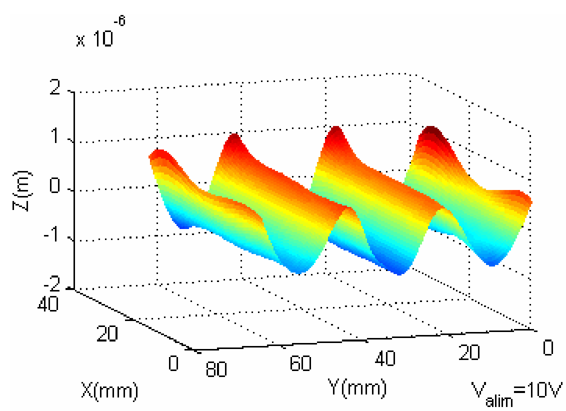

Fig.2: experimental plate deformation

On the opposite side (fig.1), four built in feet support the plate despite of hyperstaticity it implies.

Previously some studies closed to this structure [2][3] were carried out. As a difference our plate will only move normally. Indeed, as we will see later, this particular structure is not supposed to move by itself along the tangential direction. It is a passive device.

2.1 Operating principle

As explained above, feet are positioned exactly at antinodes of the standing wave induced in the plate and they are in contact with a plan steel substrate for example. Therefore, when no voltage is applied to ceramics and if users move the actuator, they can feel the classical Coulomb friction force acting at the interface feet/substrate.

When voltage is applied to ceramics electrode, however, standing wave (fig.3) is generated and we can decrease friction between feet and substrate: this happens according to amplitude vibration control. As a matter of fact, from given amplitude an intermittent contact may occur at the interface. Consequently, we create transitions between stick or slip conditions at the contact level and the global friction force changes.

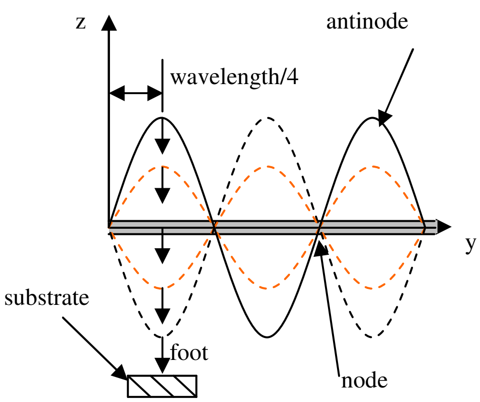

Fig.3: Stationary wave and foot trajectory

2.2 Stick/slip generation condition

From [4] micro-slip is defined as "Small relative tangential displacement in a contacting area at an interface, when the remainder of the interface in the contacting area is not relatively displaced tangentially" which means the existence of a region where surfaces are said to adhere or to stick. In our case user's action leads two surfaces in contact to slide against each other: an elastic (micro-slip) and plastic deformation may occur before macro-slip takes place.

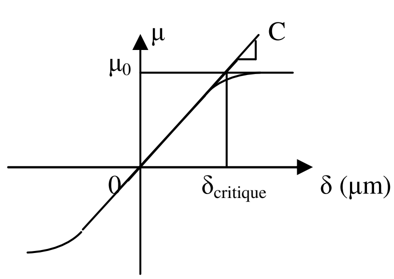

Fig.4: Coulomb- Orowan model for the friction coefficient

Therefore our principle to generate stick-slip conditions will be based on the consideration that for small displacements, foot/substrate contact presents stick and partial slip zones under a normal load Rn. Furthermore, it is shown on figure 2 that the plate deformation scale is in micrometer, so we can use an approach based on Coulomb-Orowan model (fig.4) to interpret friction coefficient variations.

Figure 4 depicts friction coefficient as a function of tangential displacement and the plot is divided approximately in two parts. The first part which relies to tangential stiffness of the contact is linear and describes the partial slip. Then, from a critical displacement (δcritic) corresponding to total slip, μ is constant.

We define δ_{critic} from the following relationship after prior identification of tangential stiffness of the foot kt:

$$\delta_{crit} = \mu_0.C.R_n = \frac{\mu_0.R_n}{k_t} \quad (1)$$

With C (m/N), the compliance and μ_0, the maximum friction coefficient at the interface.

From now, we are able to obtain μ(t) during foot/substrate contact time limited by tc and td which are respectively contact and separation instant during one period of our vibrating device. So we can write:

$$\text{if } t \in \left]t_c, t_d\right[\text{ and } \delta < \delta_c \text{ then } \quad \mu = \frac{\delta(t)}{C},$$
$$\text{if } t \in \left]t_c, t_d\right[\text{ and } \delta > \delta_c \text{ then } \quad \mu = \mu_0, \quad (2)$$

The displacement δ(t) is computed from the tangential speed integration.

2.3 Variation of normal and tangential forces

This actuator (at last one part) can be modelled as a mass-spring system as shown in figure 5.

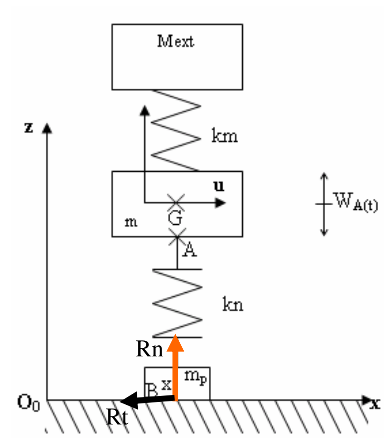

Fig. 5: Equivalent mechanical scheme and forces acting on one foot

On the figure 5, Mext represents the load applied on the top of the device to assume pre-stress. This load lies on an elastic element whose stiffness km is low so that the force Fn due to Mext is considered constant. The mass of the vibrating plate is noted m and the number of feet, n. The foot mass is too low to be considered and its normal stiffness is kn. Finally the displacement $w_A(t)$ is imposed by plate vibrations.

Applying general laws of dynamic to the system, we have:

$$\frac{m}{n}\ddot{z}_A = \frac{m}{n}\ddot{w}_A - \frac{F_n}{n} - \frac{m}{n}g + R_n(t) \quad (3)$$

Where, during contact,

$$R_n(t) = k_n(h - z_A(t)) - d_n \dot{z}_G \qquad (4)$$

And during separation,

$$R_n(t) = 0 \qquad (5)$$

The knowledge of instantaneous reaction Rn(t) by solving numerically equation 3 allows us to deduce the tangential force Rt(t). For that aim we use Coulomb's law $R_t = \mu(t) R_n$. It may be noted that μ is a function of time because we use the modelling described in figure 4, and δ is a function of time according to vibration period.

Rt mean value is obtained by integration on a vibrating period.

3 EFFECTIVENESS OF FRICTION FORCE VARIATIONS

This section is concerned with outlining friction force characteristics obtained before a preliminary device evaluation in use, in order to precise the perception limitation and to know the range for which it is available for force feedback rendering. We first need of course to illustrate the effectiveness of friction force variation controlling the excitation of the device displaced by a user.

Simulations results: So, the previous modelling has been simulated using Matlab-Simulink software®. We practised some simulations and the plots below give an overview of friction force variations. Figure 6 shows the friction force for a fixed normal pre-load equal to 20 N and different tangential speeds. It is noticeable that from a given vibration amplitude value, friction decreases suddenly. This amplitude value is due to an intermittent contact between the foot and the substrate which occurs above this given amplitude. A glass substrate (μ0=.08) was used for these trials.

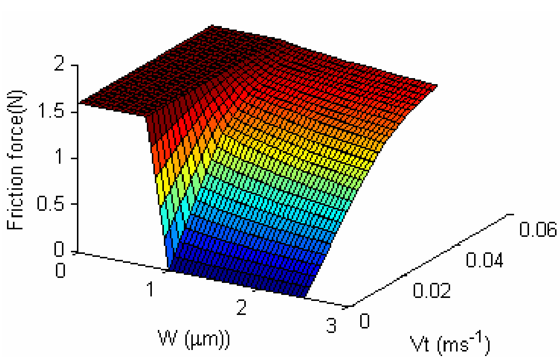

Fig. 6: Friction force on the plate at a fixed preload (simulation).

We continue our investigation and plot the graph of figure 7 observing that tangential force rises, at exploration speed of 5 cm/s with pre-load addition and decreases when the vibratory amplitude increases. We can notice that faster the plate is displaced by a user, lower friction force reduction is.

Experimental results: To compare these theoretical results to experimental one the following set-up was realised to measure friction force value. The set up consists on a cable-driven pulley system used to pull the actuator by mean of DC motor ®Maxon at a defined controlled speed. Measuring current in the DC motor, we evaluate the developed torque and then the force pulling the plate. Also, varying actuator supply voltage amplitude is equivalent to change vibratory amplitude W around 40.7 kHz. An optical encoder is mounted on the rotating shaft to count motor speed and the set up is controlled by a dSPACE DS1104.

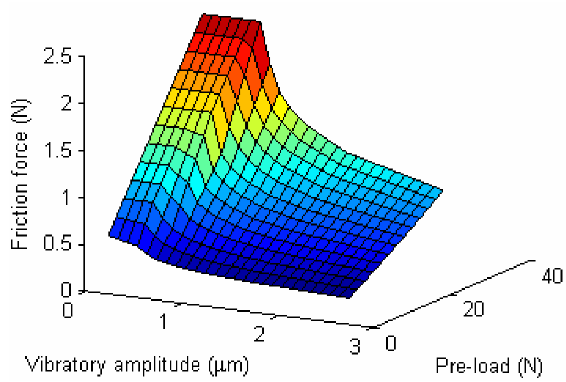

Fig. 7: Friction force on the plate at a fixed speed (simulation).

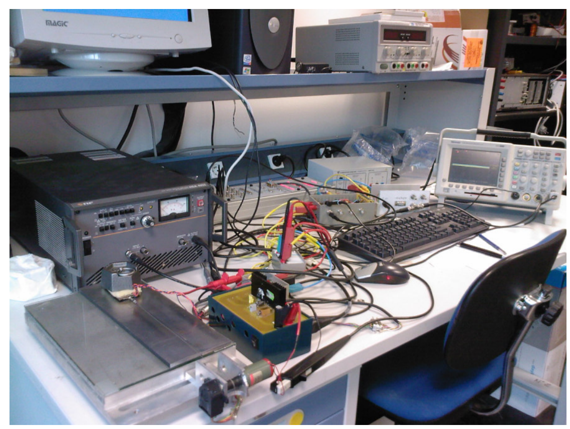

Fig 8: Experimental set up.

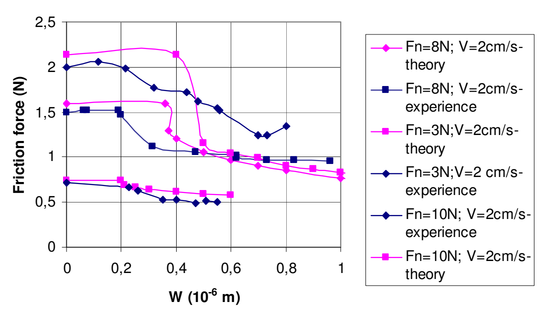

Fig 9: Theoretical and experimental results on steel surface; pre-load 3,8 and 10 N, speed 2 cm/s.

Under these conditions, figure 9 and 10 finally show some results: in particular, we have a friction force reduction which can reach 61.41 % (from .71 N to .274 N for 3 N at 1 cm/s).

Presented results enable us to see that theoretical and experimental results are close together, which tends to validate our model. More over, it may be noted that friction force is a function of the vibration amplitude. So, the vibration amplitude has to be controlled. We can also remark that this variation depends on the tangential speed imposed by the user and there will be a limitation of the effect for high speeds.

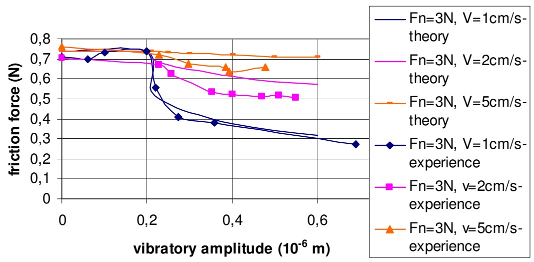

Fig. 10: Theoretical and experimental results on steel surface; pre-load 3 N, speed 1, 2 and 5 cm/s.

4 PRELIMINARY DEVICE EVALUATION

4.1 Principle of pattern simulation

The evaluation method of a haptic device is often determined by the application the device is dedicated to. And these applications highly depend on the capabilities of the haptic device. For devices working on the principle of friction reduction, typical evaluations have been performed especially in the range of cutaneous feelings rendering. From the famous Watanabe's experience [5], tactile interface designers in particular gave illusion of gratings exploration according to sliding and blocking effect alternance.

For instance, inspired by this experience, M. Biet and L. Winfield [6][7] used friction variation of a surface to simulate various textures. Indeed it can be shown that under given conditions of frequency and vibratory amplitude there's an overpressure (squeeze effect) in the air gap between two plates, one of the plates vibrating. In the works mentioned above, this principle has been used replacing one plate by the finger, the other one assuming the function of tactile device. In accordance with Watanabe's experience, vibratory amplitude was correlated with friction reduction level between the fingertip and the plate. At last, moving his finger on the vibrating plate, the user feels a sliding sensation whilst without any vibration of the plate, a sticky sensation is perceived. Then, to simulate thin textures, the idea is to control the vibration amplitude as a function of the finger position. This temporal amplitude modulation induces sliding and blocking feeling alternatively, which may be perceived as a texture [6].

As our device is also working on the principle of friction reduction but is dedicated to render reaction force on the hand, we follow the same idea to create periodic shapes. Such a result is in accordance with V. Hayward and Robles-De-La-Torre [8] who identify shape characteristics through force cues.

First we tried a simple temporal modulation of the friction coefficient at the foot/substrate interface: as expected, the result was more a vibratory sensation rather than a texture feeling. Then we replaced the temporal modulation by a spatial one to feel a sensation close to texture perception. Like M. Biet and L. Winfield for tactile devices we chose to simulate space fixed patterns shown in figure 11, which means a relationship between exploration speed and texture pattern.

To create anything like notches above, the idea is to generate alternatively sliding and blocking sensations tuning the vibrating wave amplitude.

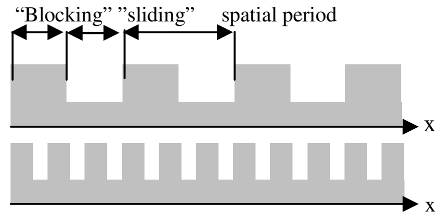

Fig. 11: texture patterns and corresponding "blocking" and "sliding" feelings.

For that, it's necessary to impose the wave amplitude reference as a function of the plate position moved by the user and measured by the optical encoder of the experimental set up. Therefore a spatial-temporal transformation allows the control of sliding region apparition times, following the kind of profiles highlighted in figure 11.

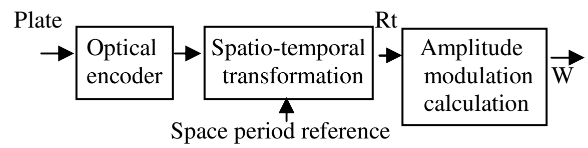

Fig. 12: wave amplitude control structure to achieve pattern simulation

On a practical point of view, to achieve this control, we modulate the amplitude of the power supply voltage with a low frequency signal on the principle schematically represented fig.12. Thus the wave amplitude modulation is controlled according to the plate position. As a result, the modulation of the vibration amplitude creates in turn a modulation of the sliding effect.

4.2 Experiments

As there is no standard for meaningful hatpic devices assessment, their evaluation implies specific tasks. It also needs to be simple enough to be easily applied while taking all important attributes of haptic interaction into account [9].

.

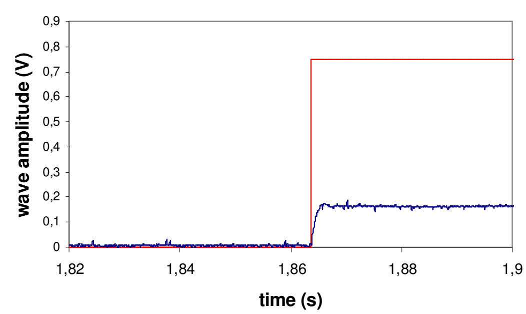

Fig.13: system wave amplitude response time

We still simulate virtual gratings depicted fig.11 generated by the device along a given distance of 87 mm, modifying spatial frequency (number of cycles) and vibration amplitude (sliding effect). The maximum number of cycles is equal to 28, that means a minimum spatial period equal to 3.1 mm. The idea is to count the spatial periods felt by the user. This procedure is quite similar to that used by West and Cutkosky [10] who asked users to count the number of 1-D sinusoidal cycles on a real and virtual surfaces, with almost the same numbers of spatial periods.

In the same time, as the device effectively provides a variable reacting force in movement, it was an opportunity to check the users ability to hold the plate, as he could do with a familiar mouse, to sense in the future the 1D boundaries or changes in form of an object displayed in a virtual environment.

But before we are going to impose vibration amplitude steps on the device. It is useful to check its wave amplitude response time. From fig.13 we can see that the preloaded plate response time of the preloaded plate is about 1 ms. Considering the typical speed with which the plate is displaced by a user, in the context of exploration, the corresponding frequency limit will never be reached.

4.3 Task and stimuli

The task required participants to move the plate on the steel substrate along the fixed distance (87 mm) and to identify the number of cycles (space frequency on fig.11) present. Two groups (respectively two and five) of graduate students were chosen to perform the experiment. Results obtained with the first group were examined before conducting additional tests with the second group. One of the subjects was female.

The experimental set up was the one described fig. 8 but the user took the place of the motor to move in forward or backward directions the device.

First of all, after presenting the “mobile” on ”rails”, subjects performed self directed displacement of the plate towards and backward to familiarise with the manipulation. Next, they were instructed to grasp the pre-load plate and to move it without voltage supply. After that the plate was excited at their unknown. From that moment they said they recognise a kind of jolts. Thereafter they were told the task consisted on counting the number of cycles present between the material limits of the displacement. We conducted some additional trials before starting the task. This preliminary stage took around 5 mns. Participants used their dominant hand and made some comments at the end of the experiment. At last, the duration of the experiment was about 30 minutes per participant.

4.4 Psychophysical results

To analyse the average results of the two groups of participants tested we present the average number of cycles (or spatial period) present for each test. We consider the result in terms of absolute value of an average error rate (DER) defined as follows [10],

$$DER = \frac{(actual\_cycles - cycles\_\det ected)}{actual\_cycles} \quad (6)$$

It’s important to notice that the wave amplitude in our experiment didn’t represent the deep of a notch, although it was the case in experiment from West and Cutkosky [10].

4.5 Experimental results

The average results obtained for both groups of subjects are graphically presented in fig.14. We have plotted average number of cycles detected for each given couple vibratory amplitude/ frequency. The symbol in the legend denotes the actual number of cycles present for the corresponding test. Each curve plots the results for a particular wave frequency (number of cycles present inside departure and arrival lines) with different points along the curve corresponding to different wave amplitudes.

Fig. 15 shows the average DER which globally isn’t greater than 12 % except at one point.

Finally, fig.16 deals with standard deviation of DER and its interpretation in fig.17 which shows the tendency to the decrease of answer range when vibratory amplitude increases.

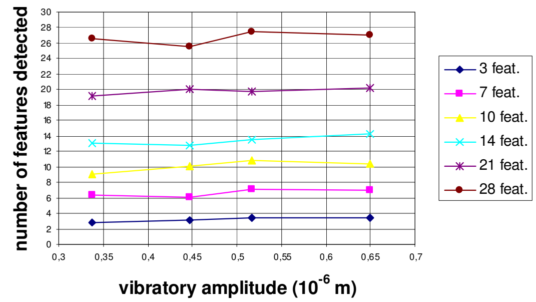

Fig. 14: average number of cycles detected

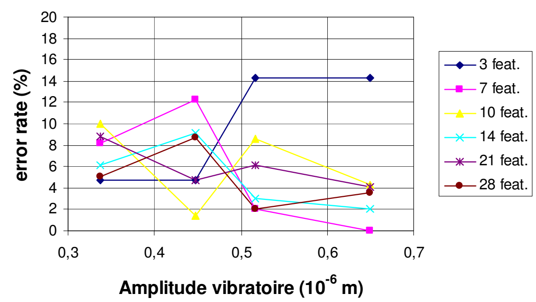

Fig.15: average error rate (DER)

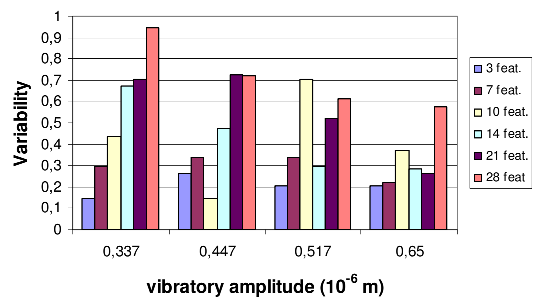

Fig. 16: standard deviation of error rate

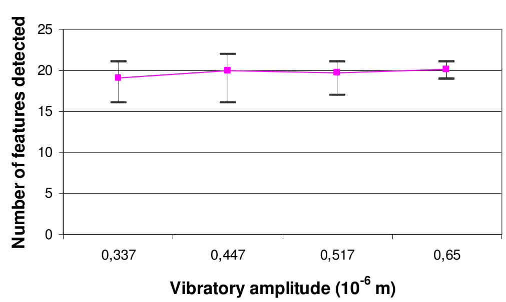

Fig. 17: interpretation of standard deviation error rate for 21 features

4.6 Discussion

An experiment of counting features in a given distance was conducted using the proposed device. Since some experimental parameters and the material differ from the one used by West and Cutkosky, we can’t directly compare our results to theirs.

Nevertheless the approach is similar and some conclusions too. We also used the DER to interpret our results. They considered that a DER of 50 % or more means that subjects are unable to count features accurately. These researchers found the arbitrary limit of 50 % to correlate well from the comments from subjects about their perceived ability to count features. They also compare the results obtained with real features. In the same manner, from us, for the range of frequencies and wave amplitudes we displayed, the DER is globally less than 12 % and participants comments didn't vary much. Also, an examination of the standard deviation of the average error rate which, in general, is lower for the tests with higher wave amplitude consolidates the idea that participants have good perception of the patterns. As a matter of the fact, almost all the participants spontaneously stated firmly to feel a "strong" sensation for the highest vibratory amplitude (.65 µm). So we can assess that the proposed device can reach physical conditions (vibration amplitude in particular) allowing accurate counting of notches.

5 CONCLUSION

In this paper we propose to use the principle of active lubrication to design a 2Dof passive haptic feedback device. The device is first described and its operating principle is explained as well. Then some details are given on the modelling of the device, leading to the expression of tangential force. Simulations are performed in order to check the effectiveness of friction control According to an experimental set-up, those simulations results are successfully compared with the simulated ones. So, it is possible to control the friction force in a range available for force feedback rendering, even if this force highly depends on normal pre-load and tangential speed. Preliminary Psycho-physic studies have been conducted to evaluate this device in use. As preliminary evaluation it trends to assess the validity of the interface for 1D low force feedback application such as assisting users for sensing the boundaries of virtual objects.

For future works and evaluation purpose, several experiments may be run to check the ability of this interface for discrimination tasks between similar Spatial Periods like in [6]: also, the shape recognition has to be investigated, according to different values of friction coefficient.

Acknowledgements

This work has been carried out within the framework of INRIA Alcove project and is supported by IRCICA (Institut de recherche sur les composants logiciels et matériels pour l' information et la communication avancée).

References

[1] L. Garbuio, J.F. Rouchon, Piezoelectric Thrust Bearing For Severe Environments, Actuator 2006, 10th International Conference On New Actuators, 14-16 June 2006, Bremen, Germany, p.185-188

[2] F. Pigache, F. Giraud and B. Lemaire-Semail, "Modelling and identification of a planar standing wave ultrasonic motor. Identification of a planar actuator", Eur. Phys. J. Appl. Phys. 34, 55-65 (2006).

[3] P. Le Moal, E. Joseph, J.C. Ferniot, "Mechanical energy transductions in standing wave ultrasonic motors: analytical modelling and experimental investigations". European Journal or Mechanics A/Solids, vol. 19, pp 849-871, 2000.

[4] Desai C.S., Zaman M.M. and Drum E.C .- Cyclinc Testing and Modelling of Interface, J.of Geotech. Eng. Vol.111, pp.793-815, 1985

[5] T. Watanabe, S. F. :a method for controlling tactile sensation of surface roughness using ultrasonic vibration, 1995 IEEE Int. Conf. on Robotics and Automation, (1995), pp 1134-1139

[6] M. Biet, G. Casiez, F. Giraud, B. Lemaire-Semail, Discrimination of Virtual Square Gratings by Dynamic Touch on Friction Based Tactile Displays, Symposium on Haptic Interfaces for Virtual Environments and Teleoperator Systems 2008, 13-14 March, Reno, Nevada, USA

[7] L. Winfield, J. Glassmire, J. E. Colgate, M. Peshkin, T-PaD: Tactile Pattern Display through Variable Friction Reduction, Second Joint Eurohaptics Conference and Symposium on Haptic Interfaces for Virtual Environment and Teleoperator Systems (WHC'07)

[8] G. Robles-De-La-Torre and V. Hayward. Force can overcome object geometry in the perception of shape through active touch. Nature, 412:445-448, 2001

[9] E. Samur, F. Wang, U. Spaetler and H. Bleuler, Generic and systematic Evaluation of Haptic Interfaces Based on Testbeds, Proc. Of the 2007 IEEE/RSJ International Conference on Intelligent Robots and Systems San Diego, CA, USA, Oct 29-Nov 2, 2007

[10]: A. M ; West and M. R. Cutkosky, Detection of real and virtual fine surface features with a haptic interface and stylus, ASME IMECE 6th Annual Symposium on Haptic Interfaces, Dallas, TX, Nov. 15-21